Yield stress modelling of doped alumina suspensions for applications in freeze granulation: towards dry pressed transparent ceramics

M. Stuer* and P. Bowen

Rheology of powder suspensions is a key factor in many processing routes, and better understanding of the parameters that control the rheology improves technical progress by reducing the empirical factors in the formulation of powder slurries. The strict requirements for the production of transparent polycrystalline alumina demand a fundamental understanding of powder handling and processing steps. The use of dopants (Mg, Y, La) has proven useful, but produces noticeable effects on suspension rheology and influences the choice of the processing route. With the prospect of spray granulation of such slurries, the rheological behaviour of doped alumina suspensions was investigated from a fundamental approach taking into account slurry and particle characteristics, and computing the interparticle potentials. This information was then used in a yield stress model which successfully predicted the rheological behaviour of the doped alumina slurries. A strategy for improved slurry formulation is presented.

Keywords: SPS, Alumina, Rheology, Freeze granulation, Modelling

This paper is part of a special issue on Novel Advanced Ceramic and Coating Processing

Introduction

Rheology represents an important aspect of many domains, including concretes, food technology, paints and pharmaceuticals, as well as ceramic processing. In particular for ceramics, suspension rheology is crucial in a variety of processing steps such as slip casting,[1–3] injection moulding,[4,5] screen printing,[6] tape casting[7] and extrusion.[8] Also for dry forming processes, the quality of the granules depends on the suspension rheology during spray drying.[9] To obtain dense and homogeneous granules, high solid load and low viscosity slurries are required. The rheology behaviour of ceramic suspensions depends on the colloidal stability, determining the degree of interaction or agglomeration of the particles.

The colloidal stability depends on the interparticle forces comprising both attractive van der Waals forces and repulsive electrostatic and steric forces.[10] Most formulations for wet ceramic processing slurries are the result of trial and error. Although efforts have been made to link the interparticle forces with slurry formulation, it is often only treated qualitatively via zeta potential or viscosity measurements.[11] Although there are many limitations with computing interparticle forces and potentials (i.e. particle shape), knowledge based progress in ceramic processing cannot proceed without understanding the key factors determining the rheological properties. A first step towards better understanding is the computation of interparticle forces (http://hamaker.epfl.ch),[12] which can be applied to the prediction of the heterocoagulation of silica and alumina slurries.[1,13]

Besides the interparticle forces, other key parameters in the rheological behaviour of ceramic suspensions include the solid load and particle shape. When solid loadings are above 30 vol.-%, ceramic slurries often show a yield stress caused by an attractive network of particles. This can be beneficial for certain forming methods such as tape casting[14] or low pressure injection moulding,[15] where a certain yield stress is desired to avoid flow after passing the high shear region. A model to predict the yield stress for concentrated particulate suspensions (YODEL)[10,16] has been recently developed and applied to cement suspensions.[17,18] It is derived from first principles taking into account interparticle forces, suspension microstructure and particle size distributions, allowing a better understanding of the key parameters controlling suspension rheology.

In this paper, we investigate the aqueous dispersion of α-Al_2O_3 powders in concentrated slurries for the freeze granulation process. The aim is to produce granules for dry pressing and subsequent sintering using pulsed electric current sintering (PECS), also referred to as spark plasma intering (SPS), to produce transparent polycrystalline alumina (PCA). Previous studies on

Powder Technology Laboratory, Material Science Institute, Swiss Federal Institute of Technology, CH-1015 Lausanne, Switzerland

*Corresponding author, email michael.stuer@epfl.ch

Published by Maney on behalf of the Institute
Received 23 August 2011; accepted 24 October 2011
DOI 10.1179/1743676111Y.0000000061

freeze dried powders have shown that doping had a beneficial effect on the real inline transmittance (RIT),[19] the best RIT being 57% compared to 86% for single crystal sapphire.[20] Other processing routes, namely, colloidal processing followed by natural sintering and post-hot isostatic pressing, have also shown very promising results, with RITs above 60%.[21,22] One of the key factors for this improvement was attributed to careful colloidal processing[23] and the elimination of any aggregates or agglomerates. However, one of the drawbacks for the application of these transparent PCAs at an industrial level is the lack of simple processing methods such as dry pressing.

Freeze drying is often used to avoid formation of aggregates on drying, but does not produce the free flowing powder needed for industrial scale dry pressing. Freeze granulation, however, has been demonstrated to be a very promising method for producing dense high quality granules with homogeneous distribution of additives.[24,25] To achieve high solid loadings and low viscosities required for freeze granulation, we have investigated the effects of different concentrations of dopants (Mg^{2+}, La^{3+}, Y^{3+}) on the slurry rheological behaviour, then used interparticle force modelling[12] along with the YODEL yield stress modelling[10,16] to provide further insight. We show that YODEL correctly models the behaviour of these ceramic slurries, allowing us to predict the rheological behaviour, improve the slurry compositions and thus the granule properties.

Materials and experimental methods

The alumina powder used in this study was a polyhedral near spherical high purity α-Al_2O_3 with a median particle size D_{v50} of 510 nm (Mastersizer S; Malvern Instruments, Malvern, UK), having a total impurity concentration of less than 0·01 mass-% ($\leqslant$5 ppm for Si, Na, Mg, Cu and Fe), a specific surface S_{BET} of 4·2 $m^2\,g^{-1}$ and an isoelectric point of 9·86 (AcoustoSizer II; Colloidal Dynamics, Warwick, RI, USA).

For the sintering experiments, doping has been introduced into the powders via dopant nitrates in suspension before freeze drying. Sintering was performed at 1350 and 1400°C by PECS (Dr Sinter 2050; Sumitomo Coal Mining Co., Tokyo, Japan), as described in detail elsewhere.[19] After mechanical polishing, thermal etching was performed in air at 1150°C for 30 min (heating rate: 10°C min^{-1}) in order to reveal the grain boundaries at the sample surface. These were then imaged in an SEM (FEG JSM-7000; JEOL, Tokyo, Japan), with the grain size distributions subsequently determined using image analysis with ImageJ and an applied grain size correction factor of 1·249 for random surface cuts through the grains.[26]

For the rheology tests, the powder was dispersed in 0·0001M HNO_3 before addition of the dopant nitrate(s), themselves also previously dissolved in 0·0001M HNO_3. After stirring and ultrasonication for 15 min of the 25 mL suspension in an ultrasonic bath, the slurries were loaded in a rheometer (RheoStress RS100; Haake, Karlruhe, Germany) using the Couette type DIN 53019 (for high viscosity) or double gap DIN 53544 (for low viscosity) setup, and kept at 25$\pm$0·1°C by a thermostatic bath. The data acquisition was performed three times on the same slurry with the same cycle with 1 min waiting time between the cycles. The cycle used was: (1) ramp from 0 to 200 s^{-1} in 90 s; (2) hold at 200 s^{-1} for 60 s; and (3) decrease from 200 to 0 s^{-1} in 90 s. The yield stress was determined using the Bingham model by taking the average on the three decreasing shear rate curves. The interaction energies are calculated using the Hamaker 2 software, selecting the non-retarded and the Hogg–Healy–Fuerstenau models for the dispersion and the electrostatic forces respectively.

Zeta potential measurements (AcoustoSizer II; Colloidal Dynamics) were performed by dispersing 4 g of powder into 156 g of 0·01M HNO_3 (2·5 wt-% suspension) and titrating over a pH range from 2 to 10 by addition of KOH. To avoid double layer compression affecting the zeta potential measurement and thereby remain close to real investigated ionic concentrations, no further electrolyte was added for the titration.

The YODEL model[10,16] was used to predict the yield stress for suspensions from first principles by taking into account interparticle forces, suspension microstructure and particle size distributions. The model predicts the yield stress using the following equation

$$\tau = m_1 \frac{\phi(\phi-\phi_0)^2}{\phi_{max}(\phi_{max}-\phi)} \quad (1)$$

where ϕ_{max} is the maximum packing of the dispersed powder, ϕ_0 is the percolation threshold and m_1 is a prefactor that accounts for particle size, particle size distribution and interparticle forces. The prefactor m_1 can be described by assuming that the contact points among particles have an average fixed radius of curvature a^*, which itself depends on the particle shape more than on the particle size. This takes into account that the interparticle forces do not simply scale with the particle size, derived for smooth spheres, and that faceted particles may have much smaller contact curvatures. m_1 can then be written as

$$m_1 = \frac{1{\cdot}8}{\pi^4} G_{max} a^* u_{k,k} \left(\frac{f^*_{\sigma,\Delta}}{R^2_{v,50}} \right) \quad (2)$$

where G_{max} is the maximum attractive interparticle force normalised by the radius of curvature at the contact points. For van der Waals attraction with a Hamaker constant A_0 and a minimum separation distance H, this can be then written as

$$G_{max} \cong \frac{A_0}{12\,H^2} \quad (3)$$

The particle size distribution is taken into account by the factors $u_{k,k}$, R_{v50} and $f^*_{\sigma,\Delta}$, described elsewhere in more detail.[10,16]

Results and discussion

Microstructural characterisation of PECS sintered PCAs

To investigate the possible reasons underlying the lower RITs found for samples sintered by PECS from freeze dried powders[19] compared to those prepared by natural sintering followed by post-HIP for colloidally produced samples,[22] microstructural analysis was performed. From the SEM images of the PECS sintered samples, it can be observed that there is a tendency for bimodal microstructures to develop, especially at higher sintering

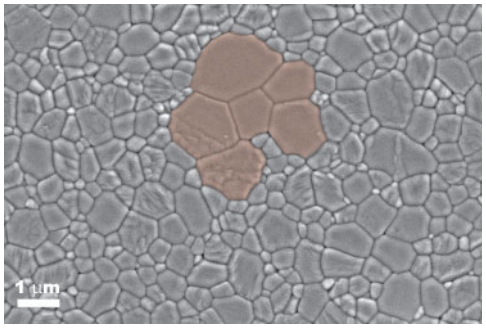

1 Microstructure of 450 ppm total cationic ratio (Mg^{2+}, La^{3+}) doped alumina sample sintered by PECS at 1400°C under 100 MPa uniaxial pressure: it can be observed that grain growth starts to be localised in spots (highlighted) surrounded by unaffected areas

temperatures. Indeed, one observes many cases in which the grain growth occurs in concentrated spots surrounded by unaffected areas with small grain sizes (Fig. 1).

The observed bimodal tendency increases with increasing sintering temperature, and is favoured by the absence of Mg^{2+} doping and/or increased grain growth, as shown in Fig. 2 for the 450 ppm (Mg^{2+}, Y^{3+}, La^{3+}) and 225 ppm (Y^{3+}, La^{3+}) doped samples sintered at 1350 and 1400°C. The signature of the bimodal characteristic are the plateaus observed in the cumulative grain size distribution curves, which are very weak at 1350°C, but more pronounced at 1400°C. In fact, at 1350°C, the sintering temperature is insufficient for extensive grain growth to occur and both microstructures are highly similar representing a small plateau at the upper grain size edge. At 1400°C, however, the thermal energy is sufficient for the system to tend towards a thermodynamic equilibrium state after full densification and grain growth, supposedly starting from the inhomogeneities caused by powder agglomeration, occurs.

To understand the origin of these microstructural trends, a particle size distribution analysis was performed on the powders before and after doping followed by

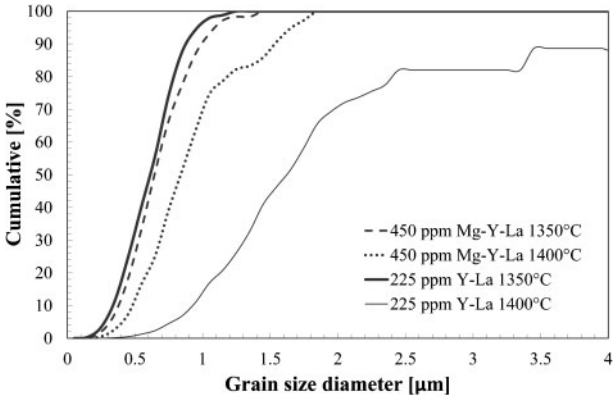

2 Cumulative grain size distribution curves for 450 ppm (Mg^{2+}, Y^{3+}, La^{3+}) and 225 ppm (Y^{3+}, La^{3+}) doped samples sintered at 1350 and 1400°C: increasing sintering temperature increases distribution range and favours bi- or multimodal grain size distributions, especially in absence of Mg^{2+} cations as indicated by plateaus in distribution curves

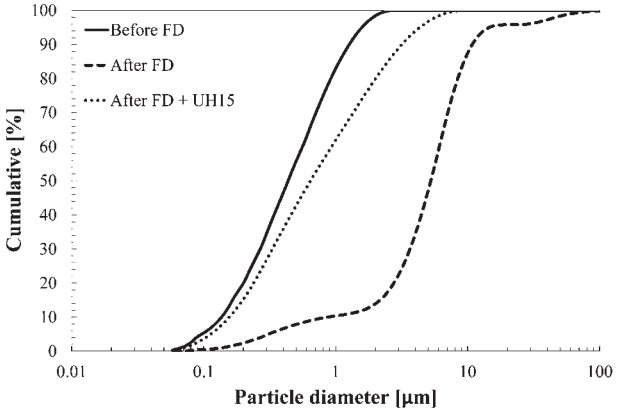

3 Cumulative powder size distribution curves before and after freeze drying (FD): powder agglomeration occurs during freeze drying, which cannot be fully reversed by 15 min ultrasonic horn treatment (UH15)

freeze drying (Fig. 3). From the cumulative particle size distributions, it can be observed that freeze granulation increases the apparent particle size by agglomeration, resulting in multimodal distributions. This heavy agglomeration can be mostly reversed during an ultrasonic horn treatment for 15 min, but the tail of the particle size distribution indicates residual agglomerates. These results suggest that particle agglomeration during freeze drying may cause inhomogeneous powder compacts and therefore, favour inhomogeneous sintering and grain growth development.

As the optical properties are dominated by the fraction of the largest grains,[27] elimination of hard agglomerates is essential. Although this could in principle be achieved by milling, the high purity required for transparent PCA excludes this possibility, instead favouring a colloidal based process. With dry pressing still in mind, we are currently investigating freeze granulation[28] for which the rheological behaviour of the powder suspensions is a key parameter. In general, highly stable and fluid suspensions are required with minimal aggregates or agglomerates and low viscosity ($<0{\cdot}25$ Pa s) at moderate shear rates (100 s^{-1}).

Rheology and modelling approach

Initial tests on the dispersion of the pure alumina showed slurries (at 35·7 wt-%) with Newtonian rheology when dispersed in nitric acid (0·0001M) at pH values between 4 and 5. Previous work, however, has shown that the use of dopants is necessary for PECS sintering of transparent PCA.[19] The effect of dopant addition in the form of nitrate salts on the rheological behaviour of alumina slurries is illustrated in Fig. 4. These results show that dopant addition increases the viscosity (higher shear stresses for the same shear rate), and also causes a yield stress to appear. This appearance of a yield stress can be interpreted as an increase in the interparticle interaction force due to the compression of the electrical double layer with the increasing ionic concentration. As expected from the Schulze–Hardy rule, the higher the cation charge at constant cationic concentration, the higher the effect on the double layer thickness and hence on the measured shear stress. The difference observed between the Mg^{2+} and the Y^{3+} or La^{3+} shear stress curves is significant, which is not the case for between the Y^{3+} and La^{3+} themselves (Fig. 4). The reasonable

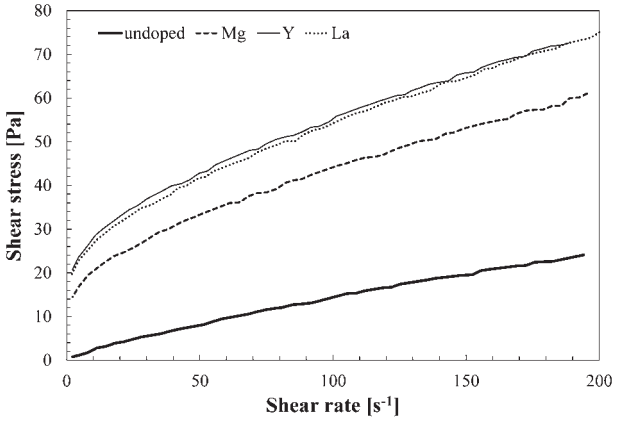

4 Effect of dopant addition (Mg^{2+}, Y^{3+}, La^{3+}) on shear stress and apparent yield stress of alumina powder dispersion in HNO_3 at pH 4 and 42 vol-% powder load: cationic dopant concentration for all of dopants is 0·0065M

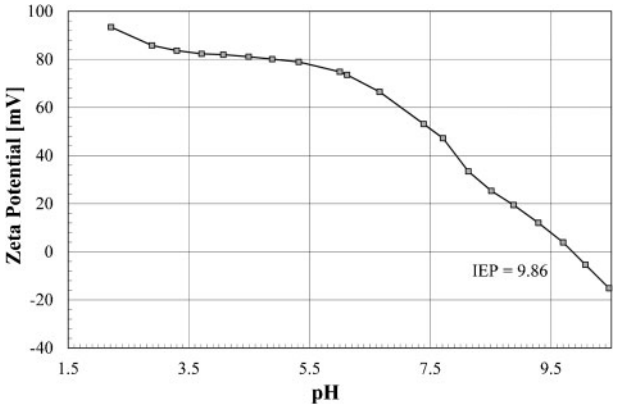

5 Zeta potential measurements by KOH 0·5M titration in 0·01M HNO_3: at pH 4, zeta potential is relatively stable around 80 mV; since total ionic concentration is very close to actual concentration in investigated powder suspensions, zeta potential value has been fixed at 80 mV for calculations

linearity of the shear stress observed beyond shear rates of 30 s^{-1} allowed us to use the Bingham model to determine the yield stress by linear extrapolation to zero shear rate.

With increasing yield stress and viscosity, freeze granulation was not possible with these doped suspensions. Mg^{2+} and Y^{3+} were selected for further analysis and to better understand and model the observed yield stresses from interparticle potential calculations[12] and the yield stress model (YODEL).[10,16] For Mg^{2+} and Y^{3+}, rheology experiments were performed at two different dopant cation concentrations for varying solid load contents, as summarised in Table 1.

In order to compare the measured yield stresses with the predictions using YODEL with the volume particle size distribution, several parameters have to be determined: (1) the Hamaker constant; (2) the minimum separation distance; (3) the contact curvature; (4) the percolation threshold; (5) the maximum packing density; and (6) the volume particle size distribution. These parameters can depend on the material, the powder, the suspension or any combination of these, and so must be specified accordingly, as enumerated below.

1. The Hamaker constant depends only on the material and suspension system, and for α-Al_2O_3 in an aqueous system has a value of $3{\cdot}67 \times 10^{-20}$ J.[29]
2. The minimum interparticle separation distance varies for each of the powder suspensions summarised in Table 1, and was assumed to be equal to the distance of the secondary minimum of the interaction energy curves. Calculating these energy curves using the Hamaker 2 software[12] requires the following data input: (a) the zeta potential; (b) the particle size; and (c) the zeta plane.
   a. the zeta potential has been experimentally measured (Fig. 5) over a range of pH levels, having a value of 80 mV at the relevant pH=4
   b. for the calculations, the D_{v50}=510 nm of the volume particle size distribution has been used as a representative value for the whole system
   c. the zeta potential plane for each suspension type was assumed to be equal to the Debye length (electrical double layer thickness),[30] calculated (Table 2) using the ionic concentrations given in Table 1.

   Using these inputs, the interaction energy results calculated by Hamaker 2[12] are plotted in Fig. 6, and the minimum separation distances obtained from the secondary minima are summarised in Table 2.
3. The distinct faceting of the powder used in this study as revealed by SEM and TEM investigations (Fig. 7) complicates the assignment of a characteristic contact curvature (CC). Since the YODEL model demands a unique characteristic value of the contact curvature, this is instead determined as a fitting parameter for a given powder slurry, with bounding values being the range observed in the SEM and TEM images. In the present case, the fitting of the YODEL predictions with the experimental yield stress values gives a contact curvature of 37 nm, which seems reasonable from the particle shape. Once the value is defined for a given powder, it is kept as a constant for modelling of other suspension conditions of the same powder.
4. The percolation threshold (PT) is another parameter which is not straightforward to determine. Variations of the percolation threshold can be, as in the present case, qualitatively verified by sedimentation tests. Higher percolation values result in larger sedimentation volumes, and *vice versa*.

Table 1 Summary of various ionic concentrations present in studied powder suspensions and their origins

Dopant	$Cation_{dopant}$/mol L^{-1}	$NO^-_{3\ dopant}$/mol L^{-1}	H^+_{acid}/mol L^{-1}	$NO^-_{3\ acid}$/mol L^{-1}	$NO^-_{3\ total}$/mol L^{-1}	Total ionic/mol L^{-1}
Mg	0·00440	0·0088	0·0001	0·0001	0·0089	0·0134
Y		0·0132			0·0133	0·0178
Mg	0·00196	0·0039			0·0040	0·0061
Y		0·0059			0·0060	0·0080

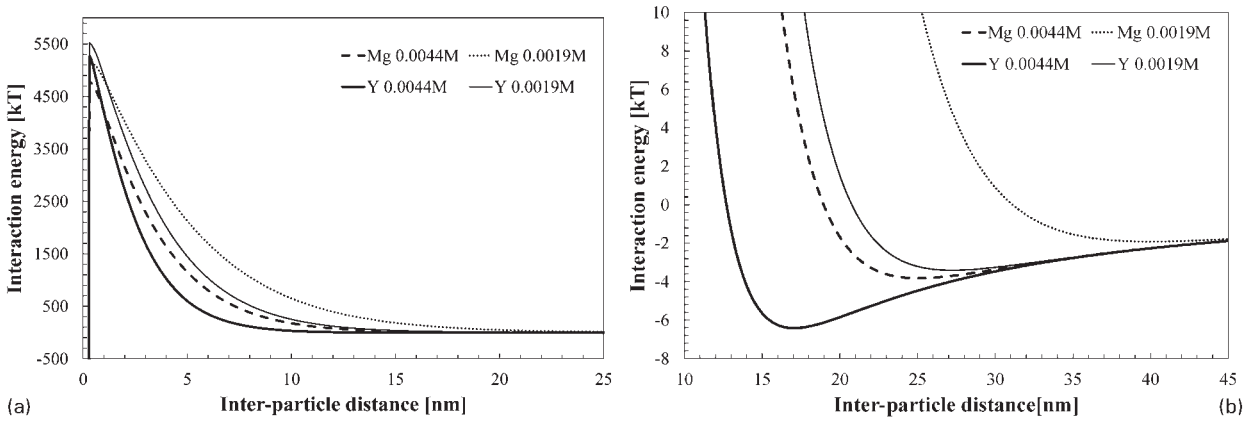

6 *a* calculated interaction energies for different powder suspension conditions: all suspensions are stable against agglomeration (cf. high energy barrier), and *b* close-up of secondary minima of interaction energies for different powder suspensions studied: increasing ionic concentrations and increasing cation charge reduce secondary minimum distance and compresses electrical double layer

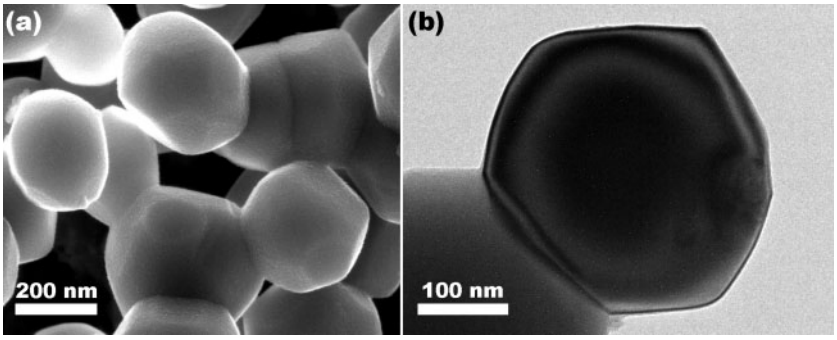

7 *a* SEM image and *b* TEM image of the powder used: it is fairly equiaxed and faceted in shape; contact curvature is difficult to estimate but is much smaller than for spherical shapes of same size; range from 30 to 60 nm represents fair estimate

However, the percolation threshold depends not purely on the powder but also on the suspension characteristics, and can therefore vary with factors such as the ionic concentration or the ionic species. In general, the PT represents the variation observed between the theoretical and practical maximum packing. Even though for one characteristic diameter of the particle size distribution (e.g. D_{v50}) the suspension is said to be stable, smaller particle fractions or particles presenting smaller contact curvature can agglomerate and thereby reduce the maximum packing. Because of the difficulties related to a correct determination of the percolation threshold, it has been used in the present study as a fitting parameter with the obtained values qualitatively verified by sedimentation tests. At 0·0044M, the sedimentation volume was 2·5 and 3·2 cm^3 for Mg^{2+} and Y^{3+} respectively, indicating a lower percolation threshold for the Y^{3+}.

5. The maximum (volume) packing (MP) density represents the theoretical maximum packing density that can be achieved with the studied powder suspension. It therefore depends only on the unagglomerated particle size distribution of the powder, as measured by laser diffraction. One way to determine the maximum packing density is to prepare green bodies by filter pressing from a perfect powder suspension. In the present study, filter pressing experiments showed that the maximum particle packing is 0·64 for dispersions in nitric acid at pH 4–5 and has been taken as a constant for all the powder suspensions.

Figure 8 illustrates the effect of the CC, PT and MP on the yield stress versus volume fraction curve for our alumina suspension. The effect of changing one parameter at a time is compared to a reference plot of CC of 50 nm, PT of 0·1 and MP of 0·6.

With increasing contact curvature, the yield stresses increase at a given volume fraction, but the ratio between the yields at different volume fractions remains relatively unchanged. Increasing the percolation threshold affects the ratio between the yields at different

Table 2 Summary of results for zeta plane used to calculate interaction energy curves and resulting minimum separation distances used for YODEL calculations

Dopant	$Cation_{dopant}$ concentration/mol L^{-1}	Debye length (zeta plane)/nm	Secondary minimum distance (minimum separation distance)/nm
Mg	0·00440	2·14	24·9
Y		1·61	17·1
Mg	0·00196	3·19	40·2
Y		2·40	27·3

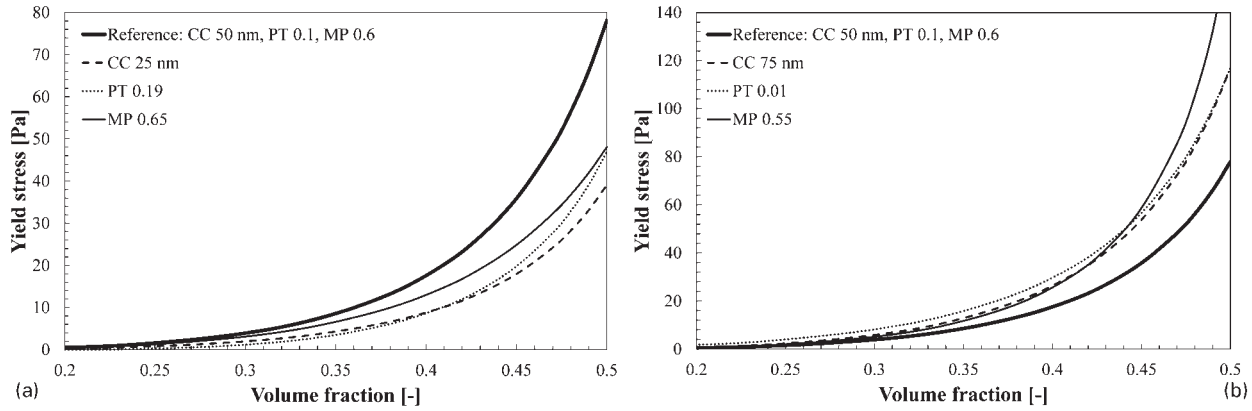

a effect of CC reduction from 50 to 25 nm, PT and MP increase from 0·1 to 0·19 and 0·6 to 0·65 respectively; *b* effect of CC increase from 50 to 75 nm, PT and MP decrease from 0·1 to 0·01 and 0·6 to 0·55 respectively

8 Suspension yield stress as function of powder volume fraction and its variation compared to reference curve with contact curvature (CC) of 50 nm, percolation threshold (PT) of 0·1 and maximum packing fraction (MP) of 0·6

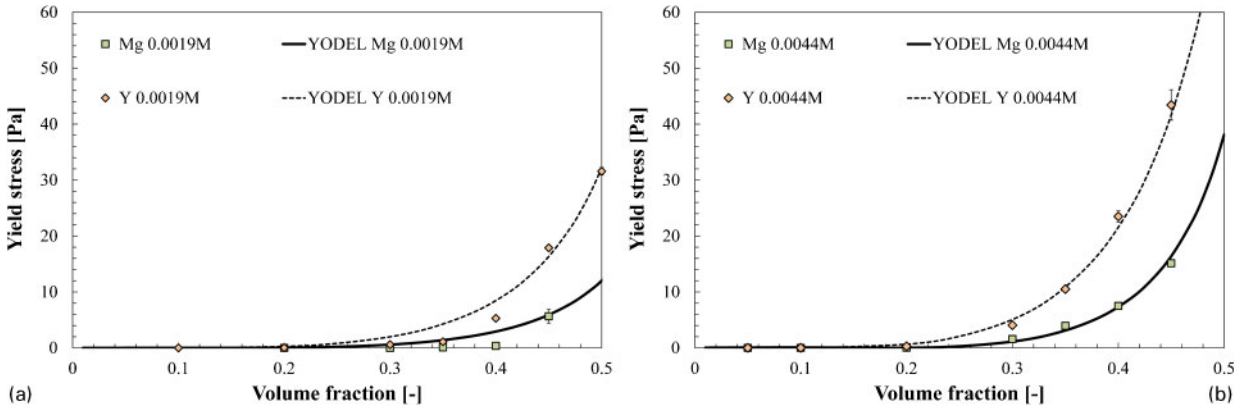

a results for Mg^{2+} and Y^{3+} at 0·0019M; *b* results for Mg^{2+} and Y^{3+} at 0·0044M

9 Experimental and modelled yield stress curves as function of powder volume fraction

volume fractions. It can be observed higher percolation thresholds flatten the curve at lower solid loads but increase the slope at higher volume fractions, i.e. more particles are required to affect the yield, but then slight changes in the solid load have increased effects. Finally, varying the maximum packing shifts the critical volume fraction (equal to the maximum packing) at which the yield rapidly increases.

Modelling results

The experimental results and the model curves are represented in Fig. 9 and the parameters used for the YODEL calculations are summarised in Table 3. The contact curvature and the maximum packing have been kept constant for all the powder slurries, and the percolation threshold was kept constant within the Mg^{2+} or Y^{3+} doped slurries respectively. With these parameters, a very good fit of the experimental data points could be obtained at 0·0044M (Fig. 9*b*) for both the Mg^{2+} and Y^{3+} powder slurries. At 0·0019M (Fig. 9*a*), the fitting is still reasonable but seems to overestimate the yield stresses at the lower volume fractions. The overall good fitting of the experimental trends with the corresponding parameters supports the applicability of the YODEL model for the predictions of the yield stresses for these alumina powder suspensions.

The decrease in the percolation threshold for the Y suspension compared to the Mg suspensions is in good agreement with the sedimentation volume tests. The results show that it is not possible to produce high volume fraction slurries with the low viscosity needed to for the preparation of dense homogenous granules in freeze drying. The normal procedure followed when electrostatic stabilisation is not possible is to instead use

Table 3 Summary of input parameters for YODEL model predictions

Dopant	$Cation_{dopant}$ concentration/mol L^{-1}	Min. separation/nm	Contact curvature/nm	Percolation threshold	Max. packing
Mg	0·00440	24·9	37	0·14	0·64
Y		17·1		0·1	
Mg	0·00196	40·2		0·14	
Y		27·3		0·1	

steric stabilisation. This route was not initially chosen in order to minimise the possible problems of carbon contamination after binder burnout, which produces poor optical properties for the PCA when using the rapid PECS sintering technique.[31]

From the interparticle energy curves, steric barriers will have to be 5–10 nm to eliminate these secondary minima and not increase the well depth. This would require relatively large molecular weight polymers adsorbed in a brush-like configuration (e.g. polyacrylic acid: 10–15 000 MW). The second alternative is to increase the ionic strength and use smaller adsorbed layers. This strategy was attempted and gave relatively satisfactory results by using PAA (2000 and 5000 MW) (ammonium salt) in basic media (pH 9–10) reducing the yield stress from above 8 Pa to below 5 Pa even with a binder and plasticiser for the dry pressing of the granules. Solid fractions were, however, limited to 30%, possibly because of Mg^{2+} complexation with the carboxylate groups of the PAA, reducing the effective adsorbed layer thickness. Currently, alternative dispersants like cross-linked and comb-like copolymers (e.g. PAA–PEG[32]) should be less sensitive to ionic strength and limit the effect of the secondary minimum.

Although the interparticle energy and yield stress modelling have helped us identify the secondary minimum as the cause of the change in the rheological behaviour, there are further steps needed to make the modelling more quantitative. The current limitations are that some of the required input parameters for the model predictions need preliminary experimental fitting of the missing parameters from several powder suspensions with varying solid loads at the required conditions.

In particular, future work on the yield stress model will focus on the effects of the suspension conditions on the maximum particle packing and the percolation threshold, in order to more accurately discern these key parameters. This will allow a step further towards accurately predicting the yield stresses with a minimum of experimental requirements.

Conclusion

Inhomogeneities in PECS/SPS sintered ceramics have been identified as being one of the limitations in the currently achieved best RITs. This was traced to the presence of hard agglomerates produced on freeze drying of the powder. Attempts to freeze granulate well dispersed slurries were prohibited by poor rheological properties when the dopants necessary for the production of transparent polycrystalline alumina were added to the slurries. Interparticle energy modelling and an existing yield stress model for suspensions (YODEL) gave an accurate fit of the experimental yield stresses. This allowed us to identify the secondary minimum of the interaction potential, brought about by the increased ionic concentration, as being the main contributor to the change in rheological properties. A strategy for the use of polymeric stabilisation was determined and at least in part successful. Further work on the several parameters used in the yield stress modelling, namely, the maximum packing fraction and percolation limit, is needed to be able to provide accurate predictions of yield stresses with a minimum of fitting or experimental input. Such a tool will be valuable in problem solving and improving the formulation of slurries for general ceramic processing.

References

1. P. Bowen, C. Carry, D. Luxembourg and H. Hofmann: 'Colloidal processing and sintering of nanosized transition aluminas', *Powder Technol.*, 2005, **157**, (1–3), 100–107.
2. F. F. Lange: 'Colloidal processing of powder for reliable ceramics', *Curr. Opin. Solid State Mater. Sci.*, 1998, **3**, (5), 496–500.
3. F. F. Lange and B. C. Yu: 'Shape forming alumina slurries via colloidal isopressing', *J. Eur. Ceram. Soc.*, 2010, **30**, (14), 2795–2803.
4. S. Novak, A. Dakskobler and V. Ribitsch: 'The effect of water on the behaviour of alumina-paraffin suspensions for low-pressure injection moulding (LPIM)', *J. Eur. Ceram. Soc.*, 2000, **20**, (12), 2175–2181.
5. W. Liu, T. Z. Bo, Z. P. Xie, Y. Wu and X. F. Yang: 'Fabrication of injection moulded translucent alumina ceramics via pressureless sintering', *Adv. Appl. Ceram.*, 2011, **110**, (4), 251–254.
6. M. D. Ger, H. W. Lin, C. P. Chang and W. H. Hwu: 'The rheological behaviors of screen-printing pastes', *J. Mater. Process. Technol.*, 2008, **197**, (1–3), 284–291.
7. F. Doreau, G. Tari, C. Pagnoux, T. Chartier and J. M. F. Ferreira: 'Processing of aqueous tape-casting of alumina with acrylic emulsion binders', *J. Eur. Ceram. Soc.*, 1998, **18**, (4), 311–321.
8. J. J. Benbow, S. Blackburn and H. Mills: 'The effects of liquid-phase rheology on the extrusion behaviour of paste', *J. Mater. Sci.*, 1998, **33**, (24), 5827–5833.
9. S. J. Lukasiewicz: 'Spray-drying ceramic powders', *J. Am. Ceram. Soc.*, 1989, **72**, (4), 617–624.
10. R. J. Flatt and P. Bowen: 'Yodel: a yield stress model for suspensions', *J. Am. Ceram. Soc.*, 2006, **89**, (4), 1244–1256.
11. E. S. Thiele and N. Setter: 'Lead zirconate titanate particle dispersion in thick-film ink formulations', *J. Am. Ceram. Soc.*, 2000, **83**, (6), 1407–1412.
12. U. Aschauer, O. Burgos-Montes, R. Moreno and P. Bowen: 'Hamaker 2: a toolkit for the calculation of particle interactions and suspension stability and its application to mullite synthesis by colloidal methods', *J. Dispers. Sci. Technol.*, 2011, **32**, (4), 470–479.
13. H. Hofmann, F. Juillerat and P. Bowen: 'Formation and drying of colloidal crystals using nanosized silica particles', *Langmuir*, 2006, **22**, (5), 2249–2257.
14. T. A. Ring: 'Fundamentals of ceramic powder processing and synthesis'; 1996, San Diego, CA, Academic Press Inc.
15. A. Dakskobler and T. Kosmac: 'Rheological properties of re-melted paraffin-wax suspensions used for LPIM', *J. Eur. Ceram. Soc.*, 2009, **29**, (10), 1831–1836.
16. R. J. Flatt and P. Bowen: 'Yield stress of multimodal powder suspensions: an extension of the YODEL (yield stress mODEL)', *J. Am. Ceram. Soc.*, 2007, **90**, (4), 1038–1044.
17. N. Roussel, A. Lemaitre, R. J. Flatt and P. Coussot: 'Steady state flow of cement suspensions: a micromechanical state of the art', *Cem. Concr. Res.*, 2010, **40**, (1), 77–84.
18. Y. F. Houst, P. Bowen, F. Perche, A. Kauppi, P. Borget, L. Galmiche, J. F. Le Meins, F. Lafuma, R. J. Flatt, I. Schober, P. F. G. Banfill, D. S. Swift, B. O. Myrvold, B. G. Petersen and K. Reknes: 'Design and function of novel superplasticizers for more durable high performance concrete (superplast project)', *Cem. Concr. Res.*, 2008, **38**, (10), 1197–1209.
19. M. Stuer, Z. Zhao, U. Aschauer and P. Bowen: 'Transparent polycrystalline alumina using spark plasma sintering: effect of Mg, Y and La doping', *J. Eur. Ceram. Soc.*, 2010, **30**, (6), 1335–1343.
20. R. Apetz and M. P. B. van Bruggen: 'Transparent alumina: a light-scattering model', *J. Am. Ceram. Soc.*, 2003, **86**, (3), 480–486.
21. A. Krell, P. Blank, H. W. Ma, T. Hutzler and M. Nebelung: 'Processing of high-density submicrometer Al_2O_3 for new applications', *J. Am. Ceram. Soc.*, 2003, **86**, (4), 546–553.
22. A. Krell, P. Blank, H. W. Ma, T. Hutzler, M. P. B. van Bruggen and R. Apetz: 'Transparent sintered corundum with high hardness and strength', *J. Am. Ceram. Soc.*, 2003, **86**, (1), 12–18.
23. A. Krell and J. Klimke: 'Effects of the homogeneity of particle coordination on solid-state sintering of transparent alumina', *J. Am. Ceram. Soc.*, 2006, **89**, (6), 1985–1992.
24. O. Lyckfeldt, D. Kack and K. Rundgren: 'Pressing and sintering developments of freeze granulated Si_3N_4 materials', *Ceram. Eng. Sci. Proc.*, 2003, **24**, (4), 331–336.
25. O. Lyckfeldt, K. Rundgren and M. Sjostedt: 'Freeze granulation for the processing of silicon nitride ceramics', *Key Eng. Mater.*, 2004, **264–268**, 281–284.
26. M. I. Mendelson: 'Average grain size in polycrystalline ceramics', *J. Am. Ceram. Soc.*, 1969, **52**, (8), 443–446.

27. C. Pecharroman, G. Mata-Osoro, L. A. Diaz, R. Torrecillas and J. S. Moya: 'On the transparency of nanostructured alumina: Rayleigh–Gans model for anisotropic spheres', *Opt. Express*, 2009, **17**, (8), 6899–6912.
28. M. Stuer, Z. Zhao and P. Bowen: 'Freeze granulation: powder processing for transparent alumina applications', *Submitted to J. Eur. Ceram. Soc.*, Special topic on transparent ceramics, 2012.
29. L. Bergstrom: 'Hamaker constants of inorganic materials', *Adv. Colloid Interface Sci.*, 1997, **70**, 125–169.
30. H. W. D. F. Evans: 'The colloidal domain: where physics, chemistry, biology, and technology meet', 672; 1999, New York, Wiley-VCH.
31. G. Bernard-Granger, N. Benameur, C. Guizard and M. Nygren: 'Influence of graphite contamination on the optical properties of transparent spinel obtained by spark plasma sintering', *Scr. Mater.*, 2009, **60**, (3), 164–167.
32. L. Bergstrom, A. M. Kjeldsen and R. J. Flatt: 'Relating the molecular structure of comb-type superplasticizers to the compression rheology of MgO suspensions', *Cem. Concr. Res.*, 2006, **36**, (7), 1231–1239.